Biodistribution and elimination pathways of PEGylated recombinant human deoxyribonuclease I after pulmonary delivery in mice

Sohaib Mahri[1,2], Aurélie Rondon[1], Tobias Wilms[1], Cynthia Bosquillon[2], Rita Vanbever[1,*]

[1] Université catholique de Louvain (UCLouvain), Louvain Drug Research Institute (LDRI), Advanced Drug Delivery & Biomaterials, Brussels 1200, Belgium.

[2] University of Nottingham, School of Pharmacy, Nottingham, UK.

*Corresponding author at: Université catholique de Louvain, Louvain Drug Research Institute, Advanced Drug Delivery and Biomaterials, Avenue Emmanuel Mounier 73, Brussels 1200, Belgium. Tel.: +32 2 764 73 25; fax: +32 2 764 73 98. E-mail address: rita.vanbever@uclouvain.be

Abbreviations

BAL, bronchoalveolar lavage; CF, cystic fibrosis; COPD, chronic obstructive pulmonary disease; DOL, degree of labelling; GI, gastrointestinal tract; IV, intravenous; MG, methyl green; MW, molecular weight; NIR, near-infrared, NIRF, near-infrared fluorescence; OD, optical density; ROI, region of interest; PBS, phosphate buffer saline; PEG, polyethylene glycol; PEG20, linear 20 kDa polyethylene glycol; PEG30, linear 30 kDa polyethylene glycol; PEG40, two-armed 40 kDa polyethylene glycol; rhDNase, recombinant human deoxyribonuclease I; SDS-PAGE, sodium dodecyl sulfate polyacrylamide gel electrophoresis; SEC, size exclusion chromatography; SEM, standard error of the mean; VT750, VivoTag-S ® 750 dye.

Abstract

Conjugation of recombinant human deoxyribonuclease I (rhDNase) to polyethylene glycol (PEG) of 20 to 40 kDa was previously shown to prolong the residence time of rhDNase in the lungs of mice after pulmonary delivery while preserving its full enzymatic activity. This work aimed to study the fate of native and PEGylated rhDNase in the lungs and to elucidate their biodistribution and elimination pathways after intratracheal instillation in mice. *In vivo* fluorescence imaging revealed that PEG30 kDa-conjugated rhDNase (PEG30-rhDNase) was retained in mouse lungs for a significantly longer period of time than native rhDNase (12 days *vs* 5 days). Confocal microscopy confirmed the presence of PEGylated rhDNase in lung airspaces for at least 7 days. In contrast, the unconjugated rhDNase was cleared from the lung lumina within 24 hours and was only found in the lung parenchyma and alveolar macrophages thereafter. Systemic absorption of intact rhDNase and PEG30-rhDNase was observed.

However, this was significantly lower for the latter. Catabolism, primarily in the lungs and secondarily systemically followed by renal excretion of byproducts were the predominant elimination pathways for both native and PEGylated rhDNase. Catabolism was nevertheless more extensive for the native protein. On the other hand, mucociliary clearance appeared to play a less prominent role in the clearance of those proteins after pulmonary delivery. The prolonged presence of PEGylated rhDNase in lung airspaces appears ideal for its mucolytic action in cystic fibrosis patients.

Keywords: Recombinant human deoxyribonuclease I, protein, PEGylation, pulmonary delivery, biodistribution, cystic fibrosis.

Graphical abstract

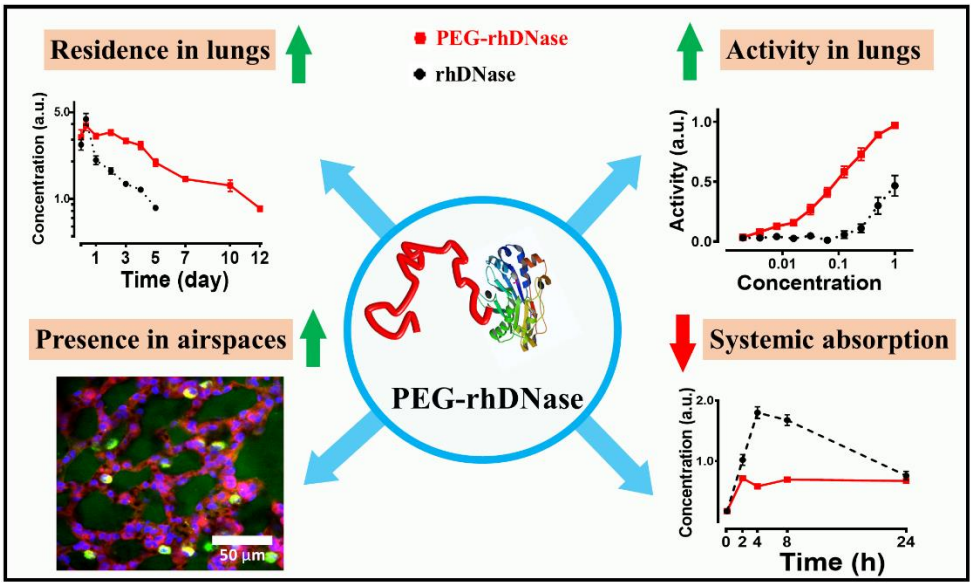

1. Introduction

Nowadays, therapeutic proteins account for more than half of the approved biopharmaceuticals and, considering their steady growth, their market share is likely to expand further in future years [1, 2]. Compared with traditional low molecular weight drugs, therapeutic proteins are endowed with higher potency and specificity, reduced toxicity and organ accumulation, and lower interaction with other drugs [3-7]. Despite obvious benefits for the topical treatment of respiratory diseases pulmonary delivery of therapeutic proteins is still in its infancy. Inhaled dornase alfa or , a mucolytic agent for the management of patients with cystic fibrosis (CF), was approved in 1993 and so far, remains the only therapeutic protein for inhalation in respiratory diseases on the market. Several other therapeutic proteins are under development for the local treatment of lung diseases such as asthma, chronic obstructive pulmonary disease (COPD), lung infections, CF or alpha-1 antitrypsin deficiency; some are in advanced stages of clinical trials [8, 9].

Proteins for inhalation face two major obstacles to successful clinical use in lung topical treatment: first, a likely physicochemical degradation during production, formulation, storage, and aerosolisation and, secondly, a short residence time in the airways [10]. Most proteins are indeed cleared from the lungs within 24 hours [11] due to the combination of effective clearance mechanisms, i.e., i) mucociliary transport towards the upper airways then elimination through the mouth and stomach, ii) absorption across lung epithelia into the systemic circulation, iii) both enzymatic and non-enzymatic degradation processes, and iv) uptake by lung cells, particularly alveolar macrophages [12-14].

Considerable efforts in the field of protein drug delivery are tailored towards increasing the half-life of short-acting proteins. A common way to achieve this goal is through conjugation to polymers, and polyethylene glycol (PEG) in particular, a strategy known as PEGylation. PEGylation, especially with high molecular weight (MW) PEGs, has proven successful in increasing the blood circulation time of proteins following injection by reducing their glomerular filtration in the kidneys, preventing enzymatic degradation, and decreasing immunogenicity [15-17].

A few studies have demonstrated a long local residence time of PEGylated proteins in the lungs following their pulmonary delivery, especially for PEG $\geq$ 20kDa [10]. The residence times were reportedly extended to at least 48 hours for linear 20 kDa (PEG20) a1-proteinase inhibitor [18], 2-arm 40 kDa PEG (PEG40) F(ab')2 and PEG40 Fab' antibody fragments compared with less

than 24 hours for their non-PEGylated counterparts [13, 19, 20]. The longer lung retention was accompanied by improved efficacy in small animal models [18, 19].

Dornase alfa or recombinant human deoxyribonuclease I (rhDNase) plays an essential role in the management of CF symptoms along with the current standard medications [21]. rhDNase decreases the viscoelasticity of respiratory secretions by cleaving the extracellular DNA primarily released by neutrophils into the airspaces [22]. However, the short residence time (< 24 hours) of rhDNase in the lungs is a considerable drawback to its full clinical benefit [23]. Therefore, prolonging its residence time in the lungs would alleviate the burden of frequent and cumbersome administrations of the drug while maintaining or even enhancing its therapeutic efficacy, thereby improving patient's life quality [10]. PEGylation of rhDNase was successfully performed with PEG20, PEG30, and PEG40 through site-specific conjugation to the N-terminal which allowed preserving the conformation and the full enzymatic activity of the protein [23, 24].

In a recent publication, pharmacokinetic studies in healthy mice following intratracheal instillation showed that 30 and 40 kDa PEG conjugates of rhDNase were present in the lungs for more than 15 days. Unconjugated rhDNase, on the other hand, had a retention of less than 24 hours. Furthermore, a single dose of PEG30-rhDNase or PEG40-rhDNase exhibited an equivalent DNA hydrolysis activity after 5 days as one daily dose of rhDNase during 5 days in β-transepithelial Na+ channel–overexpressing mice (β-ENaC) [25].

Following pulmonary administration of proteins, their clearance from the lungs might involve the mucociliary escalator towards the mouth then gastrointestinal tract (GI tract), transport across respiratory epithelia towards the bloodstream, uptake by lung cells and alveolar macrophages, and catabolism [10]. The elimination of PEGylated proteins from the lungs by systemic absorption would mean a risk of systemic toxicity, while clearance into faeces is usually synonymous with a desirable safety profile. Since rhDNase cleaves extracellular DNA in the respiratory secretions of patients with CF, it is paramount to distinguish between the ratios of enzyme in lung parenchyma (unavailable) from those in airspaces, available to exert the intended mucolytic action.

The purpose of the present work was to investigate the elimination pathways and fate of native and PEGylated rhDNase in the lungs following pulmonary delivery in mice. First, PEG20, PEG30, and PEG40 were site-specifically conjugated to rhDNase and then labelled with

different fluorochromes to be administered *via* intratracheal instillation. The fate of the native and PEGylated rhDNase compounds and PEG30 was then examined in the lungs using confocal microscopy. Finally, near-infrared fluorescence imaging (NIRF) was performed after administration of rhDNase and PEG30-rhDNase, either intratracheally or intravenously, to assess their *in vivo* biodistribution and elimination pathways.

2. Material and Methods

2.1. Materials

Commercial recombinant human deoxyribonuclease I (rhDNase, Pulmozyme®) was obtained from Genentech, Inc. (South San Francisco, CA, USA). Linear methoxy PEG propionaldehyde of 20 kDa and 30 kDa and two-arm methoxy PEG propionaldehyde of 40 kDa (PEG20, PEG30, and PEG40, respectively) were obtained from NOF Corporation (Tokyo, Japan). Alexa Fluor™ 488 TFP ester and Rhodamine B were purchased from Life Technologies (B.V., Gent, Belgium). MitoTracker® Red CMXRos, MitoTracker® Deep Red FM, and Draq5™ were purchased from Invitrogen™ (B.V., Gent, Belgium). Rhodamine-PEG30 was purchased from Creative PEGWorks (Winston Salem, NC, USA) with a degree of labelling (DOL) of Rhodamine $\geq$ 0.93. NHS-VivoTag-S ® 750 (VT750) was purchased from Perkin Elmer (Waltham, MA, USA). Unless otherwise mentioned, all other chemicals and reagents were purchased from Sigma-Aldrich (St. Louis, MO, USA).

2.2. PEGylation of rhDNase

The PEGylation of rhDNase was adapted from the method described by Guichard *et al.* [23, 25]. PEG20-rhDNase, PEG30-rhDNase, and PEG40-rhDNase were produced by conjugation of the N-terminal amino acid of rhDNase to PEG20, PEG30, and PEG40, respectively. Reductive amination in 0.1 M sodium acetate buffer (CH_3CO_2Na, pH 5) was performed using rhDNase at 10 mg/ml and a molar ratio PEG: rhDNase of 4:1 in the presence of sodium cyanoborohydride ($NaBH_3CN$) as a reducing agent (100 molar excess). The reaction mixtures were stirred at room temperature overnight. The mono-PEGylated products were purified by anion exchange chromatography on a Resource Q, 1mL column with ÄKTA™ purifier 10 system then by size exclusion chromatography (SEC) on a HiLoad 16/60 superdex 200 column (GE Healthcare Bio-Sciences AB, Uppsala, Sweden). Purification and characterisation of mono-PEGylated products are shown in Figure S1. Native and PEGylated rhDNase products were stored at 4 °C in 150 mM NaCl, 1 mM $CaCl_2$ as the marketed dornase alfa product, Pulmozyme®.

2.3. Fluorescent labelling of rhDNase and PEGylated rhDNase

Alexa Fluor™ 488 TFP ester was used for labelling rhDNase and PEGylated rhDNase products for confocal imaging experiments while NIR dye NHS-VivoTag-S ® 750 (VT750) was used for labelling rhDNase and PEG30-rhDNase for the biodistribution study by NIRF imaging. To this end, all solutions of rhDNase or PEG-rhDNases were exchanged against 1 mM $CaCl_2$ in

phosphate buffer saline (PBS) by ultrafiltration using vivaspin® Turbo 4, 3 kDa (Sartorius; Stonehouse, Gloucestershire, UK). The appropriate volume of dye at 10 mg/ml in DMSO was then added to the protein solution at a molar ratio dye: protein of 10:1 and the reaction mixtures were kept at room temperature in dark under mild agitation for 1 h. The bulk of free dye was removed by ultrafiltration using vivaspin® Turbo 15, 10 kDa MWCO (Sartorius; Stonehouse, Gloucestershire, UK). Labelled rhDNase and PEGylated rhDNase were then further purified by SEC (HiLoad Superdex 200 pg, GE, Belgium), concentrated, filtered through 0.22 μm PVDF filters, and stored at 4 °C in a solution of 150 mM NaCl and 1 mM $CaCl_2$ (Figure S2 and S3). The same degree of labelling (DOL) was achieved for all products (Table S1). The fluorescence signal of near-infrared labelled compounds was further verified by NIRF imaging (Figure S4).

2.4. Confocal imaging of mouse lungs following intratracheal instillation of PEG30 and native and PEGylated rhDNases

2.4.1. Animals

All experimental protocols were approved by the Institutional Animal Care and Use Committee of the Université catholique de Louvain (Permit number 2016/UCL/MD/019 and 2019/UCL/MD/044). 6-week old Female RjOrl SWISS mice (Elevage Janvier, Le Genest-St-Isle, France) were kept under conventional housing conditions and were allowed 1 week of acclimation before starting the experiments. Mice were fed a normal chow diet and had access to water *ad libitum*.

For intratracheal instillation, mice were anaesthetised with ketamine/xylazine (90/10 mg/kg), while for *in vivo* imaging mice were anaesthetised by 1.5–2% isoflurane (Isoflutek™, Karizoo SA, Barcelona, Spain) in oxygen.

2.4.2. Intratracheal instillation

Mice were anaesthetised by intraperitoneal injection of ketamine/xylazine (90/10 mg/kg) then fixed on an inclined board (~45°) in a supine position using surgical tape. With the aid of a small laryngoscope (Penn-CenturyTM– Model LS-2, Philadelphia, USA), mice were intubated with a 20 G catheter (VWR International BVBA, Leuven, Belgium), then 30 ± 2 µl of samples or controls were administered intratracheally into the lungs using a precision syringe (100 µl, Model 710, Hamilton, Bonaduz, Switzerland) followed by an air bolus of 200 µl using 1ml syringe (HSW SOFT-JECT®, VWR International BVBA, Leuven, Belgium). Immediately after intratracheal instillation, mice were placed in an upright position for 20-30 seconds before further studies.

2.4.3. Confocal imaging

Mice were intratracheally instilled with 1 nmol of labelled compounds (A488-rhDNase, A488-PEG20-rhDNase, A488-PEG30-rhDNase, or A488-PEG40-rhDNase). One nmol of Rhodamine B was used as a control to study the fate of the free dye. For this, Rhodamine B (MW ca. 0.48 kDa) was first dissolved in DMSO at 10 mg/ml then diluted to working solution of 16 µg/ml in 150 mM NaCl, 1 mM $CaCl_2$. One nmol (30 µl of the working solution of Rhodamine B) was then intratracheally instilled to per mouse. Likewise, 1 nmol of Rhodamine-PEG30 in 150 mM NaCl, 1 mM $CaCl_2$ (30 µl of 1 mg/ml solution) was administered intratracheally per mouse.

15 min (0.25 h), 4 h, 24 h, 48 h, 4 days, 7 days, or 15 days following administration, the mice were euthanised by cervical dislocation, and the lungs and tracheas were removed, roughly cut into ca. 2 mm slices by a razor blade then stained for confocal laser microscopy. Tissue was stained with MitoTracker® at 2 µM (MitoTracker® Red CMXRos or MitoTracker® Deep Red FM) and nuclei with either Draq5™ at 30 µM or Hoechst 33342 at 90 µM final concentration. All stains were prepared in 400 µl of 4% formaldehyde PBS solution then lung slices from the same mouse were dipped in the staining mixture for 15 min then transferred to 4% formaldehyde PBS solution until imaged. Slices were imaged within an hour using Cell Observer Spinning Disk (COSD, Zeiss, Germany) and were recorded in blue (405 nm), green (488 nm), red (561 nm), and far-red (635 nm) channels. All images were acquired at 25 magnification and stored in 16-bit format. A laser exposure time of 200 ms was used throughout the experiments.

Images were processed using ImageJ software (1.47v, NIH, USA). The detection threshold for compounds was set by choosing a cut-off so that to remove unspecific autofluorescence background (Figure S6A).

2.5. Biodistribution of rhDNase and PEG30-rhDNase in mice after intratracheal instillation

2.5.1. Longitudinal near-infrared fluorescence imaging study

Mice (6-7 per group) were intratracheally instilled with 2 nmol of VT750-rhDNase, VT750-PEG30-rhDNase, or VT750 (dye). Blank consisted of mice with no instillation. Three mice of each group were spared for the *ex vivo* study and the rest (3 to 4 mice) were imaged separately in dorsal and ventral positions at times 2-3 min, 15 min, 4 h, 8 h, and 24 h post-delivery, then every 1-3 days thereafter up to two weeks.

For the intravenous study, three mice per group were injected *via* the tail with 2 nmol of either VT750-rhDNase or VT750-PEG30-rhDNase (100 µl). Imaging was proceeded as above.

All images were acquired by an IVIS Spectrum in vivo imaging system (PerkinElmer, France) using 2D epifluorescence mode at 745/800 nm (excitation /emission) with automated exposure time and binning. Living Image® software (PerkinElmer, France) was used for image acquisition and processing. The same regions of interest (ROIs) were consistently applied to all animals (Figure 2I). The same threshold and scale (minimum to maximum) were used for comparisons among groups. The baseline fluorescence values (autofluorescence) were estimated from a group of untreated mice ($n \geq 6$) and were used to set the minimum threshold.

2.5.2. Detection of rhDNase and PEG30-rhDNase in blood, urine and faeces

Blood was collected from the tail using heparinised capillary tubes (60 µl haematocrit capillary, Hirschmann, Germany) at 2, 4, 8, and 24 h. Blood samples were imaged and ROIs were drawn around blood in microtubes. Blood samples were then centrifuged at 2500 rpm for 15 min to collect the plasma. Mice from different groups were housed in separate cages and the bedding was changed before instillation, 12 h, and 24 h post-delivery and faecal pellets were collected and imaged by IVIS Spectrum. Urines were collected at 2 h and when possible at 24 h by scuffing the mice against a metallic grid until urination then urines were collected by pipetting from a Petri dish placed underneath. Plasma and urines were frozen at -20 °C until further assayed.

2.5.3. *Ex vivo* near-infrared fluorescence imaging

Three mice of each group were sacrificed by cervical dislocation 24 h post-delivery. The blood was collected first v*ia* opened intracardiac puncture and the following organs were harvested and imaged *ex vivo*: lungs, liver, kidneys, heart, spleen, bladder, stomach, small and large intestines, and caecum. ROIs were drawn around organs placed in multiwall plates. Organs were frozen at -20 °C until further assayed.

2.5.4. SDS-PAGE gel electrophoresis of samples

Small pieces of lungs, liver, and kidneys were weighed and homogenised in 500 µl RIPA lysis buffer (Abcam, Cambridge, UK) using a tissue grinder (Polytron; Kinematica, Luzern, Switzerland). Tissue homogenates were then centrifuged at 4000 g at 4 °C for 10 min and the supernatants were stored at −20 °C. An amount of 15 µl of tissue homogenate was mixed with 5 µl of loading buffer (4x Laemmli Sample Buffer, BioRad, Belgium) then the mixture was directly loaded onto SDS-PAGE gel (4–20% Mini-PROTEAN® TGX™ Precast Protein Gels,

BioRad, Belgium). Plasma (5 µl) and urine (≤ 30 µl) samples were first diluted in PBS if needed then loaded on the gel with loading buffer (3:1 sample: loading buffer). The gels were run at 120 V for 60 min then imaged immediately by IVIS Spectrum. Known amounts of VT750-rhDNase, VT750-PEG30-rhDNase, and VT750 were loaded on each gel as controls.

2.5.5. Activity of rhDNase and PEG30-rhDNase in lung and liver homogenates

The activity of rhDNase and PEG30-rhDNase in lung and liver homogenates was assessed using the methyl green (MG) assay described earlier [23, 26]. Briefly, the hydrolysis of the DNA-Methyl Green substrate (DNA-MG) by deoxyribonuclease releases free MG in solution, the colour of this latter fades out to colourless with time leading to a decreasing optical density (OD) at 620 nm.

DNA-MG solution was prepared the day before by mixing 77% v/v of DNA from salmon testes at 2 mg/ml in buffer A (25 mM HEPES, 1 mM EDTA, pH 7.5), 4.6% of 0.4% w/v MG in buffer B (20 mM sodium acetate, pH4.2), and 18.4% of buffer C (25mM HEPES, 4 mM $CaCl_2$, 4 mM $MgCl_2$, 0.1% BSA, 0.01% thimerosal, 0.05% Tween20, pH 7.5).

Lung and liver homogenates were first diluted in buffer C (40-fold and 80-fold respectively) then further serial 2-fold dilutions of samples and controls (100 µl) were prepared in buffer C in 96-well plates. 100 µl of DNA-MG solution was added to each well and the plates were sealed and incubated in a humid chamber at 37 °C for 24 h. At the end of incubation time, the absorbance was measured at 620 nm by SpectraMax i3 (Molecular Devices, US).

2.6. Statistics

ANOVA was used for multiple group comparisons ($n \geq 3$). All data are presented as mean ± standard error of the mean (SEM). All statistical inferences are based on a two-sided significance level of * $p < 0.05$, ** $p < 0.01$, and *** $p < 0.001$ and were carried out using GraphPad Prism version 8.00 (GraphPad Software, La Jolla California USA).

3. Results and discussion

Previously published works have shown that conjugation of proteins to PEGs of MWs ≥ 20 kDa has a high potential for increasing their residence time in the lungs [13, 18-20, 27]. More recently, Guichard *et al.* demonstrated the prolonged residence time of 30 and 40 kDa PEG conjugates of rhDNase in the lungs of mice for more than 15 days compared to merely 24 h for the unconjugated rhDNase [25]. They also demonstrated the improved therapeutic efficacy of PEG30-rhDNase in β-ENaC mice, a model of the CF lung disease, as well as its safety after single and repeated administration to healthy mice. Here we investigated the biodistribution and clearance mechanisms of native and PEGylated rhDNase following pulmonary and intravenous delivery. We also showed the local fate in the lungs and provided insights into the degradation of native and PEGylated rhDNase.

3.1. Lung local distribution of native and PEGylated rhDNase

The local presence of rhDNase in airspaces is paramount for the mucolytic action of the enzyme and therefore its therapeutic efficacy. To assess the impact of PEGylation and PEG size on the local distribution of rhDNase in the lungs after pulmonary delivery, the fate of rhDNase, PEG20-rhDNase, PEG30-rhDNase, PEG40-rhDNase, PEG30, and Rhodamine was followed over time in mice by confocal microscopy.

Shortly after intratracheal instillation (15 min), all compounds were distributed to most lobes and covered many regions of the lungs. In these regions, the signal distribution in airspaces was relatively homogenous and evenly filling the airspaces with no particular accumulation pattern (Figure 1 at 0.25 h, Figure S5). The fluorescence signal from the trachea was hardly detectable even at early time points; probably due to the presence of negligible amounts or washout of compounds during the staining step. The free dye was cleared very fast on account of its low MW (~ 0.48 kDa) and hydrophobic nature as no signal was detected at 4 h in either alveolar spaces or lung cells (Figure S6B).

The signal intensity in airspaces decreased faster for rhDNase where the signal was barely detectable beyond 24 h except in alveolar macrophages and faintly in lung parenchyma. The PEGylated forms of rhDNase continued to be present in the airspaces for at least 4 days for PEG20-rhDNase and 7 days for PEG30-rhDNase and PEG40-rhDNase as well as PEG30 alone (Figures 1, S5, and S7). The fluorescent signal in alveolar macrophages was detected 4 h post instillation and persisted even after the disappearance of fluorescence from the airspaces. It

lasted 4 days for rhDNase and 15 days for PEG30-rhDNase, PEG40-rhDNase, and PEG30 alone.

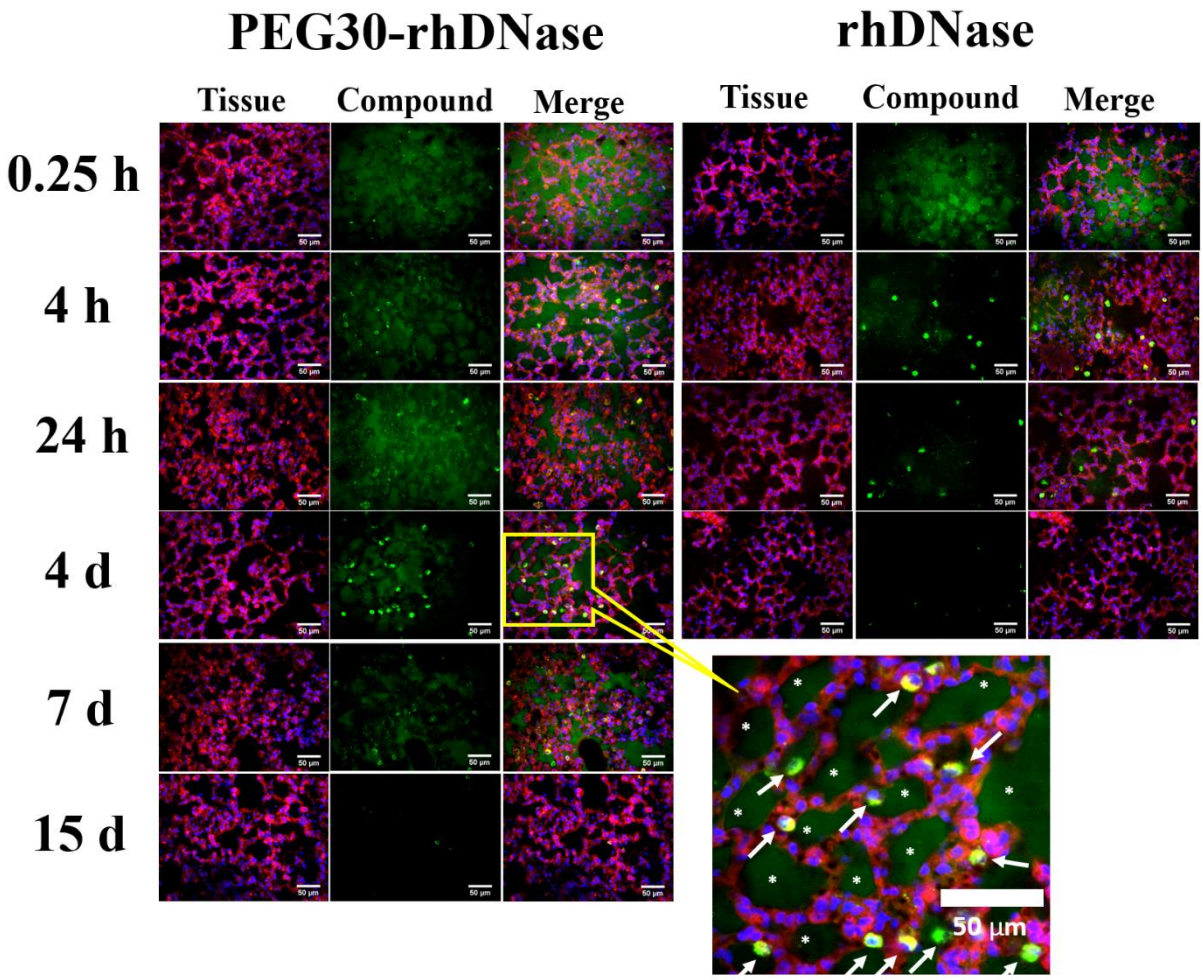

Figure 1. Representative confocal imaging of rhDNase and PEG30-rhDNase in mouse lungs. One nmol of Alexa488-rhDNase or Alexa488-PEG30-rhDNase was administered by intratracheal instillation. Mice were sacrificed at specific time points and the lungs were sliced and stained with MitoTracker® for tissue and Draq5™ for nuclei. Sections were imaged with Cell Observer Spinning Disk (COSD, Zeiss, Germany). Compounds were pseudocoloured in green, tissue in magenta, and nuclei in blue. Each experimental condition was repeated at least twice. Lower right image shows the presence of PEG30-rhDNase in alveolar macrophages (arrows →), and alveolar spaces (stars *) at day 4 post-instillation. Images were processed by ImageJ software (1.47v, NIH, USA). Scale bars, 50 µm.

The longer persistence of PEGylated rhDNase and PEG30 in alveolar macrophages compared with non-PEGylated rhDNase could be ascribed to the longer availability of the formers in the airspaces. They could also be taken up more slowly or be more resistant to degradation by alveolar macrophages [19, 27].

Numerous alveolar macrophages are actively patrolling the alveolar spaces and engulfing therapeutic particles and proteins in the epithelial lining fluid, thus considerably limiting the efficacy of pulmonary drug delivery, unless they are themselves targeted [28-30]. We suggest that the PEGylation of rhDNase could lessen its uptake by alveolar macrophages and therefore contribute to the longer retention of PEGylated rhDNase in airspaces. Overcoming the barrier of macrophage uptake through surface coating of particles with PEG was indeed shown to increase their residence time in the lungs [31]. Along this line, depleting alveolar macrophages led to a significant increase in the systemic absorption of human chorionic gonadotropin (hCG, 39.5 kDa) and IgG (150 kDa) after pulmonary administration in rats [32].

Macrophage uptake was also reported for PEG40-Fab', PEG30-rhDNase, and PEGs of up to 40 kDa after pulmonary delivery [19, 25, 27, 33]. While no quantitative data were collected in the present work, another study from our laboratory demonstrated that the uptake of PEGylated anti-IL13 Fab' by alveolar macrophages was slightly less efficient than its non-PEGylated counterpart in mice [19]. In alignment with our observations, previous work published by Freches *et al.* concluded that PEGylation delayed the clearance of Fab' fragment by alveolar macrophages and that the PEG40 moiety persisted longer than the Fab' moiety inside the cells [27].

Protection against aggregation is another likely explanation for the lower uptake of PEGylated rhDNase. Indeed, because large proteins are poorly absorbed through the lungs, they are prone to aggregation and precipitation in lung lining fluid, thus, accelerating their uptake by alveolar macrophages [34]. However, stability studies in contact with bronchoalveolar lavage (BAL) revealed that PEGylation only confers slight protection to rhDNase against aggregation and loss of activity in the absence, but not the presence, of calcium ions (Figures S8 and S9). Therefore, a potential decrease in the uptake of PEGylated rhDNase by alveolar macrophages through preventing aggregation in lung lining fluid might not be significant.

Furthermore, our data are consistent with previous work by Guichard *et al.* in which the increase in residence time of rhDNase was in accordance with the increased length of the PEG [25]. Bulkier PEGs could better protect proteins from aggregation and enzymatic degradation and reduce cell uptake and systemic absorption more efficiently [10, 25]. Patil *et al.* compared the lung retention of conjugated anti-IL-17A to PEG20 and PEG40 and nevertheless concluded that the PEG size did not affect the lung retention of anti-IL-17A to a large extent [13]. Finally, the fate of the PEG30 in mouse lungs was similar to that of the PEG30-rhDNase in terms of local

distribution pattern and retention time indicating that the fate of the PEG30-rhDNase in the lungs is highly influenced by the presence of the PEG moiety.

3.2. Lung clearance of rhDNase and PEG30-rhDNase after pulmonary delivery

Based on the confocal images and the previously published pharmacokinetic data of Guichard *et al.* demonstrating the effectiveness of PEG30-rhDNase in extending the presence of rhDNase in the lungs [25], we selected PEG30-rhDNase to carry out further biodistribution studies.

For this purpose, the NIRF signal was followed overtime after the intratracheal instillation of 2 nmol of VT750-rhDNase, VT750-PEG30-rhDNase or VT750 dye alone, in mice. As expected, the fluorescent signal was observed in the thorax immediately after instillation. The signal intensity from the ventral view was consistently higher than that from the dorsal view due to the shallower depth of the lungs from the former (Figure 2A-B). Despite being less intense, the signal from the dorsal view was less prone to interference with the signal from other organs especially at early time points (< 24 h). For instance, the fluorescent signals present in lungs, stomach and liver at 8 h post-instillation overlapped in the VT750-rhDNase group leading to an overestimation of the signal at this time point from a ventral view (Figure 2B). The contribution of other adjacent organs (i.e. the heart) to the *in vivo* apparent fluorescent signal in the thorax was negligible as was confirmed by *ex vivo* NIRF imaging at 24 h post-instillation (Figure 3A-B). It is worth mentioning that the apparent fluorescence signal detected from the lungs is underestimated compared with the signal from other relatively superficial or unprotected organs such as the liver, the stomach, and the bladder because the lungs are buried deep in the chest cavity. For instance, the dominant signal from the lungs at 24 h was only confirmed *ex vivo* (Figures 3A and B) while the *in vivo* images from the ventral view showed stronger signals from the bladder and the liver (Figure 2B). Therefore precautions should be taken when estimating relative organ distribution from live animals. Another significant drawback of the *in vivo* imaging is the presence of free dye and degraded proteins in lungs, blood, and other organs, which could bias interpretation of absorption and degradation based on *in vivo* imaging alone (see discussion below). Despite these artefacts, quantifications in live animals were useful in estimating the importance of mucociliary clearance and comparing organ distribution among groups as the *in vivo* data were in line with those obtained *ex vivo* for the lungs, liver, and digestive tract.

The fluorescence signal was present in the lungs up to 5-7 days for VT750-rhDNase and 12-14 days for VT750-PEG30-rhDNase (Figure 2A-B), in clear contrast to the VT750 dye which was cleared within 24 h (Figure S10).

Immediately after intratracheal instillation, the signal was observed in the lungs, trachea, mouth, and nose then rapidly spread throughout the whole body within 15 min indicating a systemic absorption of VT750-rhDNase, VT750-PEG30-rhDNase, and free VT750 dye (Figure 2B and Figure S10). The signal in the thorax ROI increased between time 2 min and 8 h. This artefact is ascribed to the increased signal in the blood over time, which gives rise to a higher apparent epifluorescence signal in the thorax ROI by NIRF imaging as blood vessels are located superficially beneath the surface of the skin, therefore, closer to the camera (Figure 2D). The signal in the thoracic region increased to an even higher level in the case of the VT750 dye which is absorbed more quickly due to its hydrophobic nature and low MW (i.e. 1.18 kDa *vs* 37 or 67 kDa for rhDNase or PEG30-rhDNase, respectively). Geyer *et al.* reported similar findings after pulmonary delivery of 2.5 or 10 µg of Alexa-750-siRNA to mice [35]. In that study, the fluorescence signals in the thorax increased 6 and 24 h post-delivery compared to the initial measurements for the same mice. In our case, at 24 h post-delivery and beyond, the signals in the thorax were less than those initially measured (at 2-3 min) and that of VT750-PEG30-rhDNase was 1.5 to 2-fold higher than that of VT750-rhDNase until total clearance from the lungs.

3.3. Biodistribution of rhDNase and PEG30-rhDNase after intravenous delivery

The biodistribution of rhDNase and PEG30-rhDNase after intravenous injection was also examined. Immediately after delivery, the signal was spread throughout the whole body confirming that a systemic absorption occurred after pulmonary delivery. In addition, as soon as 15 min after IV injection, a strong signal appeared in the bladder and the liver indicating a liver clearance and renal excretion of rhDNase and PEG30-rhDNase as degradation products, free dye, and intact proteins (Figure 2C), although the renal excretion of intact PEG30-rhDNase is unlikely (cf. 3.6). VT750-rhDNase did not persist in the liver for as long as VT750-PEG30-rhDNase (5 days *vs* 22 days) (Figure 2G). Moreover, *in vivo* data did not reveal any significant distribution for both compounds in other organs including the lungs. The longer half-life and liver retention of PEGylated rhDNase were expected and are likely the result of the increased protein hydrodynamic size and thereby the reduced glomerular filtration. A delayed proteolytic degradation of PEGylated rhDNase is also possible [36-39].

3.4. Organ distribution of rhDNase and PEG30-rhDNase after pulmonary delivery

Ex vivo imaging of organs at 24 h post-instillation clearly showed a dominant signal in the lungs for both VT750-rhDNase and VT750-PEG30-rhDNase groups compared to other organs (Figures 3A and B, Figures S11 and S12). The percentage of lung signal accounted for 91 ± 4% (mean ± SEM) of the total signal of harvested organs for VT750-PEG30-rhDNase compared with 66 ± 6% for VT750-rhDNase (Figure 3A and B). In addition, the total lung signal was 1.75 times higher for VT750-PEG30-rhDNase compared with that of VT750-rhDNase, consistent with the *in vivo* imaging at 24 h post-instillation (Figures 2D, 3C and 3D).

The signal in the liver peaked around 8 h and was roughly 8-fold higher in VT750-rhDNase group compared with VT750-PEG30-rhDNase at 24 h *ex vivo* (Figure 2E and Figure 3E). This is mainly attributed to the lower systemic absorption of VT750-PEG30-rhDNase preventing its significant accumulation in the liver and other distant organs. Higher signals were also detected in the heart for VT750-rhDNase compared with VT750-PEG-rhDNase ($p < 0.05$), but not in the kidneys, the spleen or the GI tract (Figure 3E).

Clearance *via* the urine seemed to be predominant for all compounds as indicated by the presence of fluorescence signal in the bladder from early time points until the total clearance of compounds from the body (Figure 2B). Nevertheless, analysis of urines showed that most of the fluorescent signal stems from the free dye and degradation products rather than intact proteins (cf. 3.6). Due to the irregularity of urination, the signal from the bladder was not used for comparison among groups and the *ex vivo* signal in the kidneys was used instead (Figures 3E and S11B). In contrast, no distinct signal from the kidneys could be obtained in live animals in Figure 2.

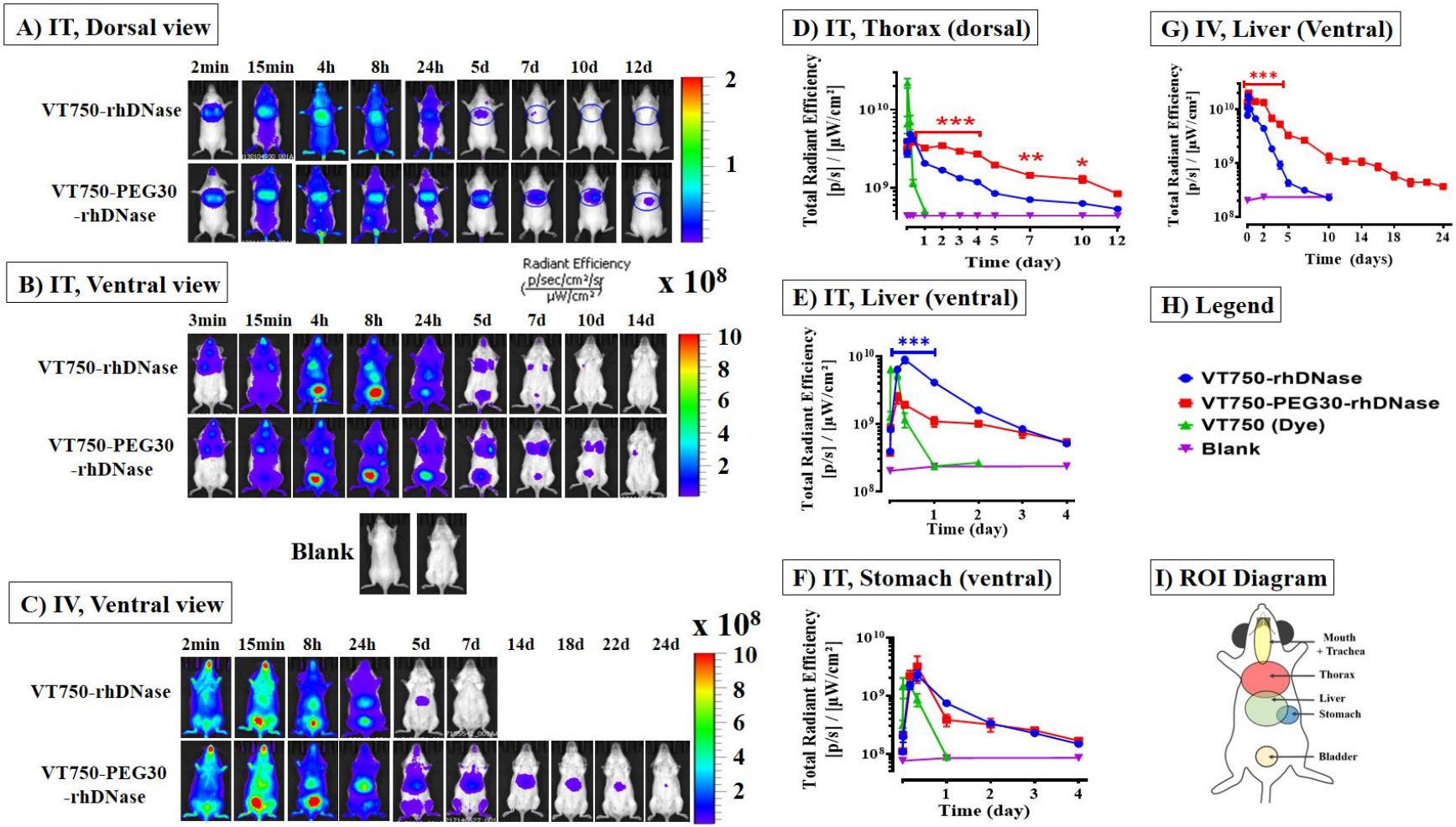

Figure 2. *In vivo* NIRF imaging in mice after intratracheal and intravenous administration. Swiss mice received 2 nmol of VT750-rhDNase, VT750-PEG30-rhDNase, or VT750 by intratracheal instillation (IT, A, B, and D-F). C and G, mice were injected intravenously (IV) *via* the tail with 2 nmol of VT750-rhDNase or VT750-PEG30-rhDNase. Blank mice did not receive any compound. Mice were imaged by IVIS Spectrum in 2D epifluorescence mode at 745/800 nm (ex/em). A and B, representative images from dorsal and ventral views, respectively after IT; D-F, quantification of ROIs in the thorax, liver, and stomach. C, representative images from ventral views after IV injection; G, quantification of ROIs in the liver. H, legend of figures D-G. I, ROI diagram. Data points represent the mean ± SEM of the total fluorescence signal (n = 3). Significant differences between VT750-rhDNase and VT750-PEG30-rhDNase are indicated by * for $p < 0.05$, ** for $p < 0.01$, and *** for $p < 0.001$ (repeated measures two-way ANOVA two-way ANOVA followed with Tukey's post hoc test).

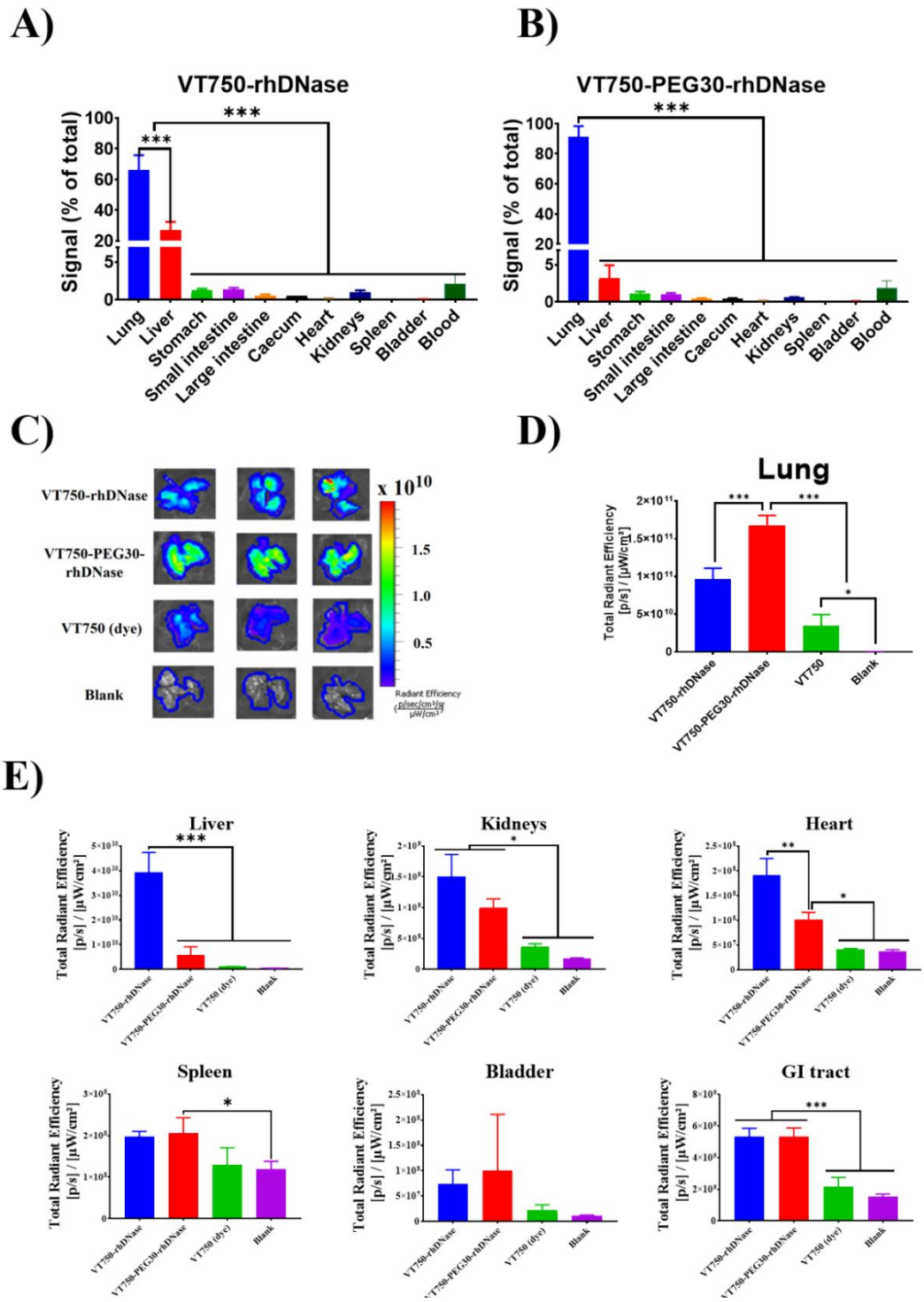

Figure 3. *Ex vivo* organ imaging in mice at 24 h post intratracheal instillation of 2 nmol of VT750-rhDNase, VT750-PEG30-rhDNase, or VT750 free dye. Mice were sacrificed, blood and organs were collected for epifluorescence quantification by IVIS Spectrum at 745/800 nm (ex/em). A and B represent the percentage of signal from each organ to the total signal from all organs for VT750-rhDNase and VT750-PEG30-rhDNase, respectively. C, NIRF images of lungs *ex vivo* and D, signal quantification ROIs in C. E, signal quantification in other organs, the GI tract signal is the sum signal from the stomach, small intestine, large intestine and caecum. Bar charts represent the mean ± SEM (n = 3). Significant differences are indicated by * $p < 0.05$, ** $p < 0.01$, or *** $p < 0.001$ (one-way ANOVA followed with Tukey's post hoc test).

On the other hand, mucociliary clearance followed by digestive elimination appeared to contribute to the clearance of rhDNase and PEG30-rhDNase after pulmonary delivery but to a low extent and indifferently according to the compound. The fluorescence signal in the stomach was not detectable at early time points (< 15 min), in contradiction with an expected rapid accumulation of compounds initially deposited in the mouth during instillation (Figure 2F). It then built up to reach a maximum at 8 h suggesting mucociliary clearance followed by swallowing occurred. It is nevertheless noteworthy that fluorescence in the stomach was easier to spot in the VT750-PEG30-rhDNase group at 4 and 8 h as the signal from the liver did not interfere at these time points (Figure 2B 8 h). The signal in the faecal pellets collected up to 24 h post instillation represented only a tiny fraction of the total signal (Figure S13) and that in the GI tract represented no more than 3% at 24 h with no difference between the VT750-rhDNase and PEG30-rhDNase groups (Figure 3E and Figure S14).

These observations support Hastings *et al.* [14] who argued that the mucociliary clearance is not a significant mechanism of protein clearance from the lungs, particularly after delivery to distal airways [13]. Its contribution could be even less effective in respiratory diseases such as chronic obstructive pulmonary disease (COPD), CF, and asthma where the mucociliary clearance is impaired [40, 41].

The longer residence time of PEGylated rhDNase compared with rhDNase in the lungs is expected to be observed if compounds were administered by nebulisation or as dry powders. In the case of nebulisation, lung deposition is more homogeneous and peripheral compared to intratracheal instillation [42]; therefore, the systemic absorption and cell uptake of both proteins are expected to be higher by nebulisation but the involvement of mucociliary clearance would be undermined. In the case of dry powder inhalers, the clearance of solid particles is driven by their physico- chemical properties; once proteins are released from their carriers in contact with lung lining fluids, the longer residence time of PEGylated rhDNase compared to rhDNase would hold due to the lower absorption and cell uptake of the former.

The pharmacokinetic advantages of PEGylated rhDNase are also expected to be observed in diseased CF lungs. Guichard *et al*. have shown that PEGylation increased the stability of rhDNase in CF respiratory secretions [24]. Moreover, the efficacy studies in β-ENaC mice showed that a single dose of PEG30-rhDNase or PEG40-rhDNase exhibited an equivalent DNA hydrolysis activity after 5 days as one daily dose of rhDNase during 5 days. These results suggest that PEGylated rhDNase was also retained longer in murine inflamed lungs [25].

3.5. Integrity of rhDNase and PEG30-rhDNase in lung homogenates

In a previous work [25], sustained retention of PEG30-rhDNase over 15 days in mouse lungs was reported, which agrees with the present data (Figure 2A-B). Nonetheless, the total clearance of unconjugated rhDNase from the lungs occurred within 24 h compared with 5 to 7 days in our experiments. To reconcile both findings, we suggest that the fluorescent signal detected for VT750-rhDNase in mouse lungs beyond 24 h might arise from degraded rhDNase in alveolar macrophages and lung parenchyma. Indeed, the signal followed by NIRF imaging originates not only from intact compounds but also from their degradation products and the released dye. It is well-established that the lungs are involved in protein metabolism, albeit to a lesser extent than the liver for example [34]. Moreover, for PEGylation to be effective as a method of improving the therapeutic efficacy of rhDNase, the enzymatic activity of PEGylated rhDNase should be preserved *in vivo*. It was therefore important to investigate the integrity and enzymatic activity of rhDNase and PEG30-rhDNase in the lungs.

Gel electrophoresis of lung homogenates revealed the presence of distinct bands corresponding to the intact proteins as well as byproducts of VT750-rhDNase and VT750-PEG30-rhDNase at 24 h (Figure 4A and B). The intensity of the bands corresponding to intact VT750-PE30-rhDNase was 18.9 ± 1.0% of the total signal, 10-fold higher than that of VT750-rhDNase (1.8 ± 0.4%) (Figure 4A-C). This is in correlation with the 10-fold higher enzymatic activity on DNA of VT750-PEG30-rhDNase in lung homogenates compared with VT750-rhDNase (Figure 4D).

Bands corresponding to the released VT750 dye and rhDNase fragments of roughly estimated MWs between 10 and 20 kDa were detected in lung homogenates for both VT750-rhDNase and VT750-PEG30-rhDNase groups (arrows in Figure 4A). Interestingly, no bands corresponding to the MW of rhDNase (~37 kDa) were visible for the VT750-PEG30-rhDNase group. The band observed just below that of VT750-PEG30-rhDNase likely corresponds to the same fragments of rhDNase (10-20 kDa) still attached to the PEG30 moiety (Figures 4A and B). The most plausible explanation is that the degradation of the protein moiety in PEG30-rhDNase occurs first, while still attached to the PEG, which is then followed by the cleavage of the PEG moiety [42].

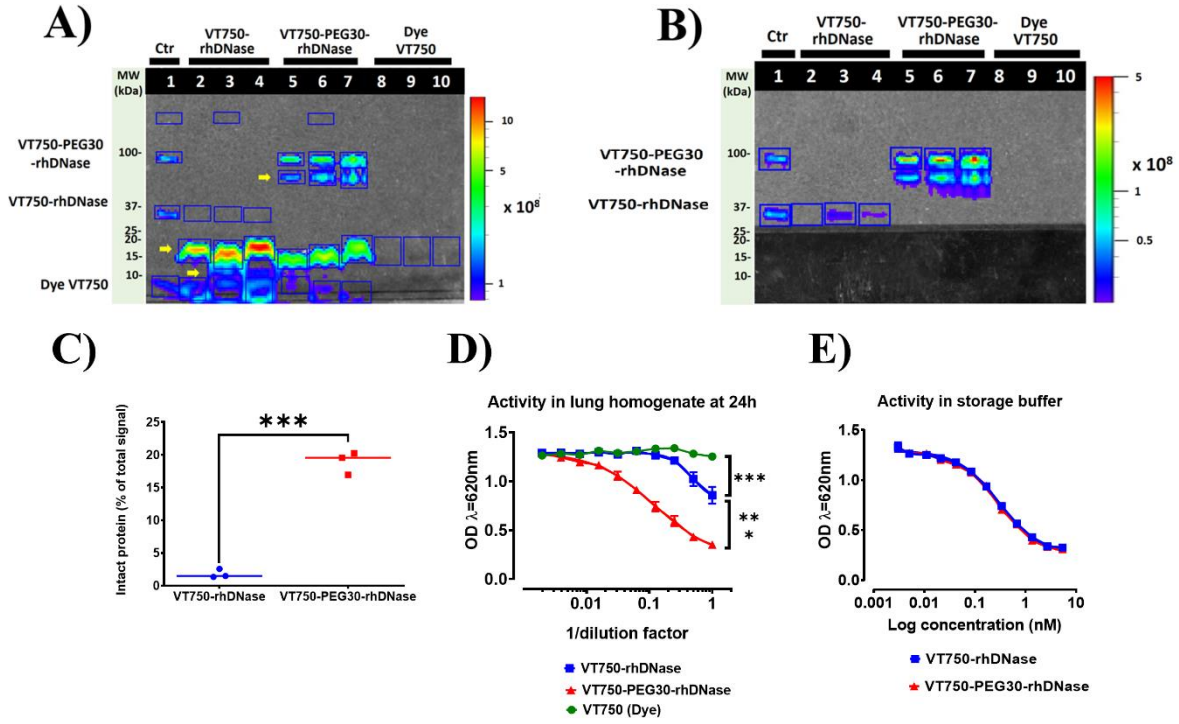

Figure 4. *Ex vivo* analysis of lung homogenates 24 h post instillation of 2 nmol of VT750-rhDNase, VT750-PEG30-rhDNase, or VT750 (dye). A) SDS-PAGE of lung homogenates, arrows point to degradation fragments. B) Same image as A after concealing the bottom part of the gel and amplifying the signal to visualise VT750-rhDNase bands. Lane 1, Control loaded with VT750-rhDNase (~10 ng), VT750-PEG30-rhDNase, and VT750; Lanes 2-10, samples from different mice. Gel was imaged by IVIS Spectrum (745/800 nm ex/em). Scale in radiant efficiency ([p/s/cm²/sr] / [µW/cm²]). C) Percentage of signal intensities of intact bands to the total signal intensity of all bands in the same lane. D) Enzymatic activity of lung homogenates on DNA-MG substrate. E) Enzymatic activity of stock solutions of VT750-rhDNase and VT750-PEG30-rhDNase, showing their similar enzymatic activity. DNA hydrolysis releases MG in solution leading to a decrease in the absorbance at 620 nm after 24 h of incubation at 37 °C. Data represent mean ± SEM (n = 3, t-test (C) and two-way ANOVA followed with Tukey's post hoc test (D-E), ** $p < 0.01$, and *** $p < 0.001$). MW, molecular weight.

The degradation of the protein moiety of PEGylated proteins was demonstrated by Elliot *et al.* who followed the fate of PEG40-insulin in the plasma of rats after intravenous administration [43]. Using antibodies directed against PEG (anti-PEG) and insulin (anti-insulin), they detected the PEG moiety over a much longer period of time than insulin by Western blot but could not detect the native unmodified insulin, therefore, concluded that insulin was most likely degraded while still coupled to the PEG moiety, losing, thus, its antigenic epitopes.

Our data suggest that PEG30-rhDNase suffered less degradation in the lungs and, therefore, retained more activity compared with rhDNase, which was extensively degraded at 24 h.

Taken together with the confocal images (Figure 1) and the pharmacokinetic data of Guichard *et al.* [25] in which rhDNase was cleared from the lungs within 24 h, it is likely that the intact fractions of rhDNase and PEG30-rhDNase in lung homogenates at 24 h are localised extracellularly whereas the intracellular signal observed in alveolar macrophages and epithelial cells by confocal imaging corresponds mostly to degraded fragments.

3.6. Systemic absorption of rhDNase and PEG30-rhDNase after pulmonary delivery

Systemic absorption to the bloodstream is another clearance mechanism of proteins from the lungs besides mucociliary clearance and local degradation. The systemic absorption of rhDNase after a single inhalation has been shown to range from less than 2% in monkeys up to 15% in rats [44]. Proteins of similar or larger MWs such as human chorionic gonadotropin (hCG, 39.5 kDa), human albumin (68 kDa), and IgG (150 kDa) have also been reported to be absorbed into the blood after pulmonary delivery, albeit poorly [32, 34]. However, a few studies have reported a decrease in lung absorption of proteins upon their PEGylation. Following pulmonary delivery in rats, the bioavailability of recombinant human granulocyte-colony stimulating factor (rhGCSF, 18 kDa) dropped threefold after conjugation to 6 kDa PEG (11.9% to 4.5%) and even lower after conjugation to 12 kDa PEG (1.6%)[45]. A similar decrease was observed for IFNα2b (19 kDa), with its bioavailability reduced from 15% to 5.5% and < 0.4% when conjugated to PEGs of 12 kDa and 40 kDa, respectively [7]. Patil *et al.* showed that PEGylation of anti-IL-13 and anti-IL-17A (47 kDa) with PEG40 reduced both their uptake and transport across Calu-3 human lung epithelial cells [13]. Based on these studies and the general assumption that larger proteins are less absorbed from the lungs [7, 46], PEGylation was expected to diminish the absorption of rhDNase across the lung epithelial barrier.

Systemic absorption of both VT750-rhDNase and VT750-PEG30-rhDNase was suspected from observations in live animals and isolated organs (Figure 2 and Figure 3). This was confirmed by monitoring the presence of the proteins in the blood. The maximum blood signals of VT750-rhDNase were higher than those of VT750-PEG30-rhDNase (Figure 5A and Figure S15). The absorption of intact compounds was confirmed by the presence of bands corresponding to MWs of both intact VT750-rhDNase and VT750-PEG30-rhDNase in plasma by gel electrophoresis (Figure 5B). The signal of VT750-rhDNase in the blood peaked at around 4 h post-delivery then decreased slowly thereafter, whereas that of VT750-PEG30-rhDNase increased initially then remained relatively steady from 2 h to 24 h. The signal intensity patterns of VT750-rhDNase and VT750 PEG30-rhDNase bands in plasma were overall in agreement with the

signals from the whole blood. However, the signal in the blood from 4 h onwards might be influenced more by the presence of free dye and degradation products rather than intact proteins. Indeed, besides the free dye detected in all groups, faint bands corresponding to degraded fragments of VT750-rhDNase and VT750-PEG30-rhDNase similar to those detected in lung homogenates at 24 h were detected in plasma between 4 h and 24 h (Figure 5B). These degradation fragments likely diffused from the lungs into the systemic circulation. However, degradation of VT750-rhDNase and VT750 PEG30-rhDNase could also have occurred in plasma, liver or other tissues after systemic absorption.

Gel electrophoresis of urine samples collected 2 h after intratracheal instillation showed the presence of intact VT750-rhDNase but not VT750-PEG30-rhDNase (Figure 5C). Renal excretion of VT750-rhDNase is expected to be relatively rapid due to the low MW of rhDNase compared with the threshold of renal filtration (60-70 kDa) [39, 47-50]. On the other hand, no traces of intact VT750-PEG30-rhDNase could be detected in the urine at 2 h and 24 h, likely due to its large molecular volume (Figure 5C and Figure S16). Our measurements of the hydrodynamic size of rhDNase and PEG30-rhDNase by dynamic light scattering indicate a size of ~ 4.8 nm for rhDNase and ~10 nm for PEG30-rhDNase (Table S2). The hydrodynamic size of the latter is larger than that of serum albumin (68 kDa, ~ 6 nm), a protein of similar MW [51]. It is known that the molecular size of PEGylated proteins is much larger than proteins of similar MWs [39, 52]. In fact, the hydrodynamic volume of PEG 18 kDa alone is greater than that of serum albumin [53]. Therefore, the renal filtration of intact PEG30-rhDNase should in principle be negligible. It is worthwhile to mention that PEGs as big as 40 kDa were shown to be excreted in the urines of mice, rats, and humans [54-56].

No bands of either VT750-rhDNase or VT750-PEG30-rhDNase could be detected in the kidneys which could be also explained by the weak signal obtained in the kidneys ex vivo at 24 h (Figure S17). Only degraded fragments of VT750-rhDNase were detected in the liver for VT750-rhDNase group at 24 h, suggesting the potential implication of the liver in the catabolism of the protein after absorption from the lung. On the other hand, the signal intensity in the liver was too low to detect any bands for the VT750-PEG30-rhDNase group (Figure S17).

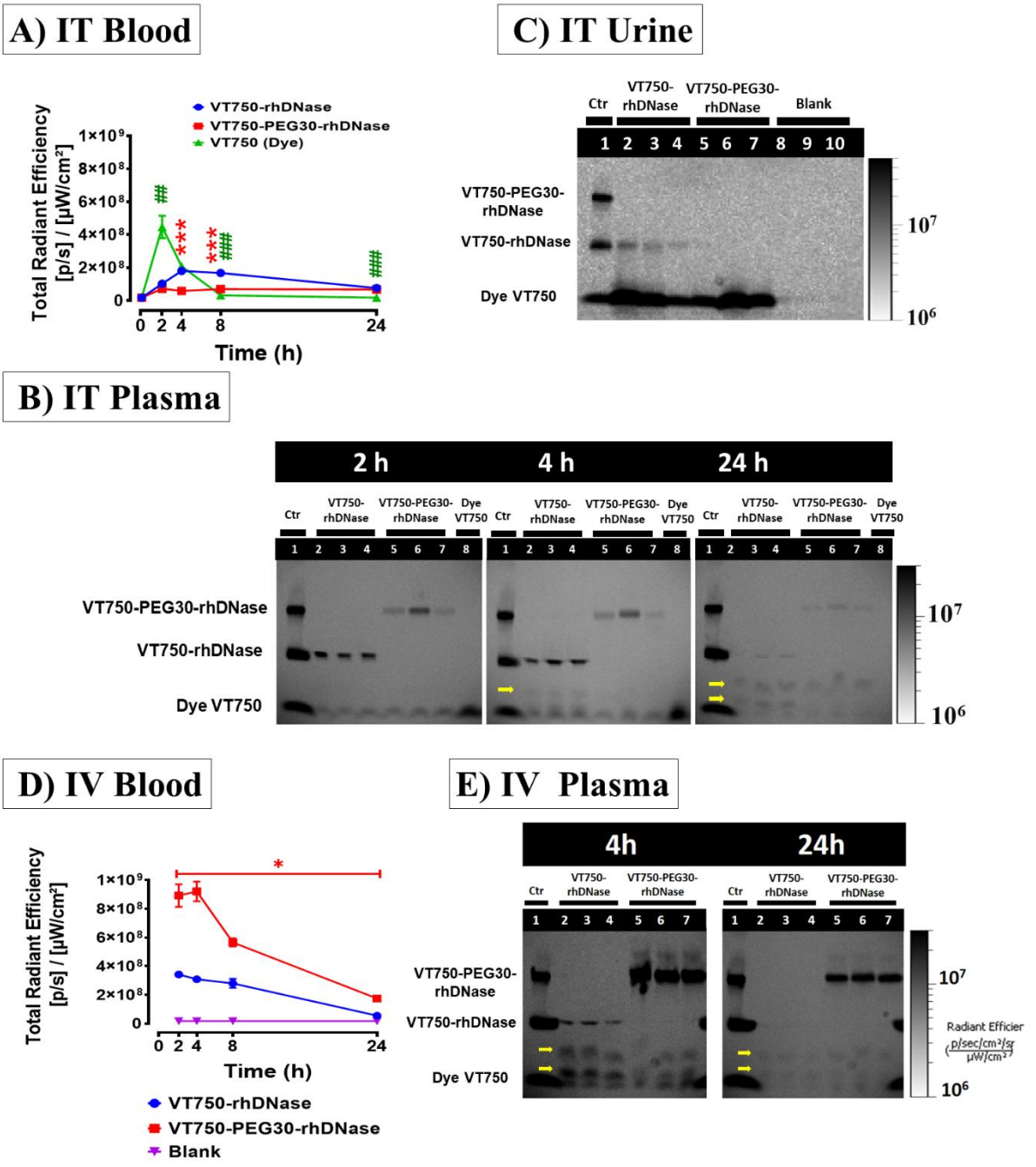

Figure 5. Analysis of blood, plasma, and urine by NIRF imaging. Mice received 2 nmol of VT750-rhDNase, VT750-PEG30-rhDNase, or VT750 by intratracheal instillation (IT, A-C) or intravenous injection (IV, D and E). **A, D)** Quantification of signal in blood samples collected at 2, 4, 8, and 24 h post-delivery by IVIS Spectrum at 745/800 nm (ex/em). **B)** SDS-PAGE of plasma (5 µl) at 2, 4, and 24 h post-instillation. **C**) SDS-PAGE of urines (30 µl) collected at 2 h post-instillation. **E**) SDS-PAGE of plasma (5 µl) at 2 and 24 h post-injection. Arrows point to degradation fragments. Samples were mixed with loading buffer (3:1 sample: 4x Laemmli) then loaded on the gel (4–20%) and run at 120 V for 60 min. Lane 1, Control loaded with VT750-rhDNase (~10 ng), VT750-PEG30-rhDNase, and VT750; Samples from different mice are in lanes 2-8 (B), 2-10 (C), or 2-7 (E). Gels were imaged by IVIS Spectrum (745/800 nm ex/em). Scale in radiant efficiency ([p/s/cm²/sr] / [µW/cm²]). Data points represent the mean ± SEM (n = 3). Significant differences from VT750-rhDNase are indicated by *** $p < 0.001$ for VT750-PEG30-rhDNase and ### $p < 0.001$ for VT750 (two-way ANOVA followed with Tukey's post hoc test).

3.7. Elimination of rhDNase and PEG30-rhDNase after intravenous delivery

After IV injection, VT750-rhDNase was cleared from the blood faster than VT750-PEG30-rhDNase (Figure 5D). Plasma concentrations of VT750-rhDNase were already lower than those of VT750-PEG30-rhDNase at 2 h and were barely detectable at 24 h (Figure 5D-E). Gel electrophoresis of plasma collected 4 h and 24 h post-injection showed similar degradation products for both VT750-rhDNase and VT750-PEG30-rhDNase (Figure 5E). These degradation products are also similar to those found in the plasma 24 h post-instillation (Figure 5B). This confirms our earlier suggestion that further degradation in the plasma, liver, or other tissues could occur following systemic absorption of both intact and degraded rhDNase and PEG30-rhDNase from the lungs.

4. Conclusions

In this work, the fate in the lungs and elimination pathways of native and PEGylated rhDNase were investigated following intratracheal delivery to healthy mice. Native rhDNase was cleared from the lungs within 24 h whereas conjugation to PEGs of 20 to 40 kDa sustained the presence of the enzyme in lung airspaces for more than 4 days (PEG20-rhDNase) or 7 days (PEG30-rhDNase and PEG40-rhDNase) after a single dose. Reduced degradation within the lungs and lower systemic absorption were identified as major mechanisms driving the longer retention of PEGylated rhDNase in the lungs. Both rhDNase and PEG30-rhDNase were primarily degraded in the lungs and secondarily in the blood, liver, or other tissues, followed by renal excretion of byproducts. Interestingly, the degradation of PEG30-rhDNase likely involves an initial fragmentation of the protein followed by a detachment of the PEG moiety. Following intratracheal instillation, no accumulation of the proteins was seen in other organs at the exception of rhDNase in the liver. However, liver accumulation was prominent after IV injection and was more marked for PEG30-rhDNase. Alveolar macrophages were shown to actively take up both PEGylated and native rhDNase as well as PEG alone. More in-depth mechanistic studies are being conducted to determine the influence of PEGylation on the uptake by macrophages, the transport across lung epithelial cells, and the interaction with respiratory mucus. Overall, the prolonged presence of PEGylated rhDNase in lung airspaces would be ideal for its mucolytic action in patients with CF.

Acknowledgements

The authors would like to thank Donatienne Tyteca and Patrick Van Der Smissen from de Duve Institute (UCLouvain, Brussels) for kindly providing advice and MitoTracker® dyes for confocal microscopy, Bernard Ucakar for his help with the biodistribution studies. This work was a thesis project funded by the European Commission, Education, Audiovisual and Culture Executive Agency (EACEA), Erasmus Mundus programme, NanoFar doctorate (EMJD NanoFar - ref.520170-1-2011-1-FR-ERA MUNDUS-EMJD). This work was also supported by a complementary scholarship "bourse de Patrimoine", UCLouvain, Belgium. Rita Vanbever is Research Director of the Fonds National de la Recherche Scientifique (Belgium).

Conflicts of interest

The authors report no conflict of interest.

References

1. Walsh, G., *Biopharmaceutical benchmarks 2014.* Nature Biotechnology, 2014. **32**(10): p. 992-1000.
2. Walsh, G., *Biopharmaceutical benchmarks 2018.* Nat Biotechnol, 2018. **36**(12): p. 1136-1145.
3. Marx, V., *Watching peptide drugs grow up.* Chemical & Engineering News, 2005. **83**(11): p. 17-+.
4. Renukuntla, J., et al., *Approaches for enhancing oral bioavailability of peptides and proteins.* International Journal of Pharmaceutics, 2013. **447**(1-2): p. 75-93.
5. Agyei, D., et al., *Protein and Peptide Biopharmaceuticals: An Overview.* Protein and Peptide Letters, 2017. **24**(2): p. 94-101.
6. Leader, B., Q.J. Baca, and D.E. Golan, *Protein therapeutics: A summary and pharmacological classification.* Nature Reviews Drug Discovery, 2008. **7**(1): p. 21-39.
7. McLeod, V.M., et al., *Optimal PEGylation can improve the exposure of interferon in the lungs following pulmonary administration.* J Pharm Sci, 2015. **104**(4): p. 1421-30.
8. de Kruijf, W. and C. Ehrhardt, *Inhalation delivery of complex drugs - the next steps.* Current Opinion in Pharmacology, 2017. **36**: p. 52-57.
9. Bodier-Montagutelli, E., et al., *Designing inhaled protein therapeutics for topical lung delivery: what are the next steps?* Expert Opinion on Drug Delivery, 2018. **15**(8): p. 729-736.
10. Guichard, M.J., T. Leal, and R. Vanbever, *PEGylation, an approach for improving the pulmonary delivery of biopharmaceuticals.* Current Opinion in Colloid & Interface Science, 2017. **31**: p. 43-50.
11. Todoroff, J. and R. Vanbever, *Fate of nanomedicines in the lungs.* Current Opinion in Colloid & Interface Science, 2011. **16**(3): p. 246-254.
12. Villegas, M.R., A. Baeza, and M. Vallet-Regi, *Nanotechnological Strategies for Protein Delivery.* Molecules, 2018. **23**(5).
13. Patil, H.P., et al., *Fate of PEGylated antibody fragments following delivery to the lungs: Influence of delivery site, PEG size and lung inflammation.* Journal of Controlled Release, 2018. **272**: p. 62-71.

14. Hastings, R.H., H.G. Folkesson, and M.A. Matthay, *Mechanisms of alveolar protein clearance in the intact lung.* American Journal of Physiology-Lung Cellular and Molecular Physiology, 2004. **286**(4): p. L679-L689.
15. Werle, M. and A. Bernkop-Schnurch, *Strategies to improve plasma half life time of peptide and protein drugs.* Amino Acids, 2006. **30**(4): p. 351-67.
16. Veronese, F.M. and A. Mero, *The impact of PEGylation on biological therapies.* BioDrugs, 2008. **22**(5): p. 315-29.
17. Pasut, G. and F.M. Veronese, *State of the art in PEGylation: the great versatility achieved after forty years of research.* J Control Release, 2012. **161**(2): p. 461-72.
18. Cantin, A.M., et al., *Polyethylene glycol conjugation at Cys232 prolongs the half-life of alpha1 proteinase inhibitor.* Am J Respir Cell Mol Biol, 2002. **27**(6): p. 659-65.
19. Koussoroplis, S.J., et al., *PEGylation of antibody fragments greatly increases their local residence time following delivery to the respiratory tract.* Journal of Controlled Release, 2014. **187**: p. 91-100.
20. Freches, D., et al., *PEGylation prolongs the pulmonary retention of an anti-IL-17A Fab' antibody fragment after pulmonary delivery in three different species.* Int J Pharm, 2017. **521**(1-2): p. 120-129.
21. DeSimone, E., et al., *Cystic Fibrosis Update on Treatment Guidelines and New Recommendations.* Us Pharmacist, 2018. **43**(5): p. 16-21.
22. Shak, S., et al., *Recombinant human DNase I reduces the viscosity of cystic fibrosis sputum.* Proc Natl Acad Sci U S A, 1990. **87**(23): p. 9188-92.
23. Guichard, M.J., et al., *Production and characterization of a PEGylated derivative of recombinant human deoxyribonuclease I for cystic fibrosis therapy.* International Journal of Pharmaceutics, 2017. **524**(1-2): p. 159-167.
24. Guichard, M.J., et al., *Impact of PEGylation on the mucolytic activity of recombinant human deoxyribonuclease I in cystic fibrosis sputum.* Clin Sci (Lond), 2018. **132**(13): p. 1439-1452.
25. Guichard, M.J., et al., *PEGylation of recombinant human deoxyribonuclease I provides a long-acting version of the mucolytic for patients with cystic fibrosis.* Advanced Therapeutics. In press.
26. Sinicropi, D., et al., *Colorimetric determination of DNase I activity with a DNA-methyl green substrate.* Anal Biochem, 1994. **222**(2): p. 351-8.
27. Freches, D., et al., *Preclinical evaluation of topically-administered PEGylated Fab' lung toxicity.* Int J Pharm X, 2019. **1**: p. 100019.
28. Lombry, C., et al., *Confocal imaging of rat lungs following intratracheal delivery of dry powders or solutions of fluorescent probes.* J Control Release, 2002. **83**(3): p. 331-41.
29. Hastings, R.H., et al., *Cellular uptake of albumin from lungs of anesthetized rabbits.* Am J Physiol, 1995. **269**(4 Pt 1): p. L453-62.
30. Lehnert, B.E., *Pulmonary and thoracic macrophage subpopulations and clearance of particles from the lung.* Environmental health perspectives, 1992. **97**: p. 17-46.
31. Shen, T.W., et al., *Distribution and Cellular Uptake of PEGylated Polymeric Particles in the Lung Towards Cell-Specific Targeted Delivery.* Pharm Res, 2015. **32**(10): p. 3248-60.
32. Lombry, C., et al., *Alveolar macrophages are a primary barrier to pulmonary absorption of macromolecules.* Am J Physiol Lung Cell Mol Physiol, 2004. **286**(5): p. L1002-8.
33. Gursahani, H., et al., *Absorption of Polyethylene Glycol (PEG) Polymers: The Effect of PEG Size on Permeability.* Journal of Pharmaceutical Sciences, 2009. **98**(8): p. 2847-2856.
34. Patton, J.S., C.S. Fishburn, and J.G. Weers, *The lungs as a portal of entry for systemic drug delivery.* Proc Am Thorac Soc, 2004. **1**(4): p. 338-44.
35. Geyer, A., et al., *Fluorescence- and computed tomography for assessing the biodistribution of siRNA after intratracheal application in mice.* Int J Pharm, 2017. **525**(2): p. 359-366.
36. Kozlowski, A., S.A. Charles, and J.M. Harris, *Development of pegylated interferons for the treatment of chronic hepatitis C.* BioDrugs, 2001. **15**(7): p. 419-29.

37. Fletcher, A.M., et al., *Adverse vacuolation in multiple tissues in cynomolgus monkeys following repeat-dose administration of a PEGylated protein.* Toxicology Letters, 2019. **317**: p. 120-129.
38. Zbyszynski, P., et al., *Probing the subcutaneous absorption of a PEGylated FUD peptide nanomedicine via in vivo fluorescence imaging.* Nano Convergence, 2019. **6**.
39. Caliceti, P. and F.M. Veronese, *Pharmacokinetic and biodistribution properties of poly(ethylene glycol)-protein conjugates.* Advanced Drug Delivery Reviews, 2003. **55**(10): p. 1261-1277.
40. Rogers, D.F., *Physiology of airway mucus secretion and pathophysiology of hypersecretion.* Respiratory Care, 2007. **52**(9): p. 1134-1149.
41. Whitsett, J.A., *Airway Epithelial Differentiation and Mucociliary Clearance.* Annals of the American Thoracic Society, 2018. **15**(Suppl 3): p. S143-S148.
42. Tibbitts, J., et al., *Key factors influencing ADME properties of therapeutic proteins: A need for ADME characterization in drug discovery and development.* Mabs, 2016. **8**(2): p. 229-245.
43. Elliott, V.L., et al., *Evidence for Metabolic Cleavage of a PEGylated Protein in Vivo Using Multiple Analytical Methodologies.* Molecular Pharmaceutics, 2012. **9**(5): p. 1291-1301.
44. Tandel, H., K. Florence, and A. Misra, *9 - Protein and Peptide Delivery through Respiratory Pathway*, in *Challenges in Delivery of Therapeutic Genomics and Proteomics*, A. Misra, Editor. 2011, Elsevier: London. p. 429-479.
45. Niven, R.W., et al., *The pulmonary absorption of aerosolized and intratracheally instilled rhG-CSF and monoPEGylated rhG-CSF.* Pharm Res, 1995. **12**(9): p. 1343-9.
46. Patton, J.S., *Mechanisms of macromolecule absorption by the lungs.* Advanced Drug Delivery Reviews, 1996. **19**(1): p. 3-36.
47. Buchanan, A. and J.D. Revell, *Chapter 8 - Novel Therapeutic Proteins and Peptides*, in *Novel Approaches and Strategies for Biologics, Vaccines and Cancer Therapies*, M. Singh and M. Salnikova, Editors. 2015, Academic Press: San Diego. p. 171-197.
48. Turecek, P.L., et al., *PEGylation of Biopharmaceuticals: A Review of Chemistry and Nonclinical Safety Information of Approved Drugs.* Journal of Pharmaceutical Sciences, 2016. **105**(2): p. 460-475.
49. Veronese, F.M. and G. Pasut, *PEGylation, successful approach to drug delivery.* Drug Discov Today, 2005. **10**(21): p. 1451-8.
50. Mitragotri, S., P.A. Burke, and R. Langer, *Overcoming the challenges in administering biopharmaceuticals: formulation and delivery strategies.* Nature Reviews Drug Discovery, 2014. **13**(9): p. 655-672.
51. Hushcha, T.O., A.I. Luik, and Y.N. Naboka, *Conformation changes of albumin in its interaction with physiologically active compounds as studied by quasi-elastic light scattering spectroscopy and ultrasonic method.* Talanta, 2000. **53**(1): p. 29-34.
52. Niven, R.W., et al., *PULMONARY ABSORPTION OF POLYETHYLENE GLYCOLATED RECOMBINANT HUMAN GRANULOCYTE-COLONY-STIMULATING FACTOR (PEG RHG-CSF).* Journal of Controlled Release, 1994. **32**(2): p. 177-189.
53. Sherman, M.R., et al., *Conjugation of high-molecular weight poly(ethylene glycol) to cytokines: Granulocyte-macrophage colony-stimulating factors as model substrates*, in *Poly(Ethylene Glycol): Chemistry and Biological Applications*, J.M. Harris and S. Zalipsky, Editors. 1997. p. 155-169.
54. Parton, T., et al., *P-0167: The PEG Moiety of Certolizumab Pegol is Rapidly Cleared From the Blood of Humans by the Kidneys Once it is Cleaved From the Fab'.* Inflammatory Bowel Diseases, 2009. **15**(suppl_2): p. S56-S56.
55. Longley, C.B., et al., *Biodistribution and excretion of radiolabeled 40 kDa polyethylene glycol following intravenous administration in mice.* Journal of Pharmaceutical Sciences, 2013. **102**(7): p. 2362-2370.
56. Parton, T., et al., *P068 Investigation of the Distribution and Elimination of the PEG Component of Certolizumab Pegol in Rats.* Journal of Crohn's and Colitis Supplements, 2008. **2**(1): p. 26-26.